© 2017. Published by The Company of Biologists Ltd | Journal of Experimental Biology (2017) 220, 1701-1708 doi:10.1242/jeb.156109

RESEARCH ARTICLE

Regional differences in the preferred e-vector orientation of honeybee ocellar photoreceptors

Yuri Ogawa[1,2,*], Willi Ribi[3], Jochen Zeil[3] and Jan M. Hemmi[1]

ABSTRACT

In addition to compound eyes, honeybees (*Apis mellifera*) possess three single-lens eyes called ocelli located on the top of the head. Ocelli are involved in head-attitude control and in some insects have been shown to provide celestial compass information. Anatomical and early electrophysiological studies have suggested that UV and blue–green photoreceptors in ocelli are polarization sensitive. However, their retinal distribution and receptor characteristics have not been documented. Here, we used intracellular electrophysiology to determine the relationship between the spectral and polarization sensitivity of the photoreceptors and their position within the visual field of the ocelli. We first determined a photoreceptor's spectral response through a series of monochromatic flashes (340–600 nm). We found UV and green receptors, with peak sensitivities at 360 and 500 nm, respectively. We subsequently measured polarization sensitivity at the photoreceptor's peak sensitivity wavelength by rotating a polarizer with monochromatic flashes. Polarization sensitivity (PS) values were significantly higher in UV receptors (3.8±1.5, *N*=61) than in green receptors (2.1±0.6, *N*=60). Interestingly, most receptors with receptive fields below 35 deg elevation were sensitive to vertically polarized light while the receptors with visual fields above 35 deg were sensitive to a wide range of polarization angles. These results agree well with anatomical measurements showing differences in rhabdom orientations between dorsal and ventral retinae. We discuss the functional significance of the distribution of polarization sensitivities across the visual field of ocelli by highlighting the information the ocelli are able to extract from the bee's visual environment.

KEY WORDS: Ocelli, Polarization vision, Retina fine structure

INTRODUCTION

Most insects possess two or three dorsal ocelli, small single-lens eyes that are situated on top of the head, in addition to their compound eyes. Even though the optics of ocelli generate relatively low-resolution images, the superior speed and sensitivity of ocelli, compared with the compound eyes, means that they can improve the visual performance of insects by complementing and modulating compound eye functions (Mizunami, 1995). Ocelli are especially important for the control of head orientation around the roll and pitch axes in some species (Wilson, 1978; Stange, 1981; Taylor, 1981; Mizunami, 1995), by detecting movement relative to the horizon (e.g. Stange et al., 2002; Berry et al., 2006, 2007a,b,c). They are particularly important at low light levels (Wellington, 1974; Berry et al., 2011). Ocelli have also been shown to be involved in providing compass information by sensing the pattern of polarized skylight (Wellington, 1974; Fent and Wehner, 1985). Anatomically, the cross-sections of ocellar rhabdoms in many hymenopteran insects are straight and are formed by microvilli from two photoreceptors that are positioned opposite to each other. This arrangement and the fact that the rhabdom sheets do not twist along their length indicates that they are likely to be polarization sensitive (Kral, 1978; Ribi et al., 2011; Zeil et al., 2014). A recent study of the particular alignment of elongated rhabdoms in the three ocelli of orchid bees has provided further evidence for the possible involvement of ocelli in the detection of polarized skylight (Taylor et al., 2015). In contrast, the cross-sections of ocellar rhabdoms in the nocturnal bee *Megalopta* are not straight (Ribi et al., 2011) and the ocellar photoreceptors have indeed been found not to be polarization sensitive (Berry et al., 2011). The polarization sensitivity in ocelli has been suggested not only to provide celestial compass information but also to improve segmentation of the horizon line by enhancing contrast for the control of head attitude, particularly around roll and pitch axes (Zeil et al., 2014). However, to date, only two electrophysiological investigations have provided evidence that ocellar photoreceptors are polarization sensitive in the desert ant, *Cataglyphis bicolor* (Mote and Wehner, 1980), and in the honeybee, *Apis mellifera* (Geiser and Labhart, 1982), but no information is available about the distribution of preferred e-vector sensitivity across the visual field of the ocelli.

The three dorsal ocelli of honeybee workers, *A. mellifera*, are placed in a triangular arrangement on top of the head. The median ocellus is located in the centre and faces forward, while the two lateral ocelli look sideways. Each lateral ocellus contains approximately 1100 photoreceptors and the median ocellus consists of 1350 photoreceptors (W.R., unpublished data). Each ocellar retina is divided into distinct dorsal and ventral sub-retinae (Ribi et al., 2011). Using intracellular recordings in honeybee ocelli, Geiser and Labhart (1982) identified UV receptors with a spectral sensitivity maximum at 345 nm with a secondary peak at 490 nm and blue–green receptors maximally sensitive to wavelengths of 490 nm. They also reported that the UV receptors have a higher polarization sensitivity (PS) value (4.7±2.5) compared with the blue–green receptors (1.7±0.6). However, the relationship between spectral sensitivity and preferred e-vector orientation of photoreceptors remains unclear as is their distribution across the ocellar retina. Recently published retinal maps of ocellar rhabdom orientations have revealed interesting patterns of uniform and non-uniform distributions in hymenopteran ocelli (e.g. Ribi et al., 2011; Zeil et al., 2014; Taylor et al., 2015).

Here, we investigated the relationship between the spectral and polarization sensitivity of photoreceptors and their receptive field

[1]School of Biological Sciences and UWA Oceans Institute (M092), The University of Western Australia, 35 Stirling Highway, Crawley, WA 6009, Australia. [2]Department of Biological Sciences, Macquarie University, Sydney, NSW 2109, Australia. [3]Research School of Biology, The Australian National University, Canberra, ACT 2601, Australia.

*Author for correspondence (yuriogawa.kato@mq.edu.au)

Y.O., 0000-0002-9708-7063

Received 9 January 2017; Accepted 15 February 2017

Journal of Experimental Biology (2017) 220, 1701-1708 doi:10.1242/jeb.156109

positions with respect to the visual horizon. Our results agree with previous findings that UV photoreceptors have a higher polarization sensitivity compared with green-sensitive receptors. We also demonstrate that the preferred e-vector orientation of photoreceptors differs depending on whether their optical axes lie in the dorsal or the ventral visual field, regardless of whether they are UV or green receptors. Our results suggest that the distribution of polarization sensitivity across the visual field of ocelli reflects their dual role in providing input to both the head attitude control and the celestial compass system.

MATERIALS AND METHODS

Animals

Electrophysiology was performed on honeybee foragers (*Apis mellifera* Linnaeus 1758) collected on the Crawley campus of the University of Western Australia, Perth. Bees caught at a hive at the Australian National University in Canberra were used for histology.

Electrophysiology

Animals were chilled on ice for 6 min and their legs were then removed. Bees were subsequently fixed to a plastic stage with beeswax, dorsal side up, so that the head orientation was always vertical. The plastic stage was oriented horizontally for recordings from the dorsal and ventral retinae in the median ocelli. However, it was tilted by ±30 deg around the bee's longitudinal axis in order to access the photoreceptors in the ventral retinae of the lateral ocelli. Monochromatic stimulation lights were produced by computer-controlled Till Polychrome V monochromators (Till Photonics GmbH, Gräfelfing, Germany) with 150 W xenon lamps. A 1 mm optical fibre attached to a Cardan arm perimeter device, which is pointing at its centre of rotation, delivered the light to the eye. The diameter of the exit point of the fibre subtended 4 deg as seen from the bee's perspective. The quantum flux of each monochromatic stimulus was measured by a radiometer (ILT1700, International Light Technologies, Peabody, MA, USA) and the number of photons was adjusted to be equal between 340 and 600 nm using a neutral density wedge (NDC-50C-4, Thorlabs Inc., Newton, NJ, USA).

A bee was mounted at the centre of rotation of the perimeter device, allowing selective illumination of either the lateral or the median ocellar lens. A borosilicate glass microelectrode filled with 1 mol l^{-1} potassium chloride with a resistance of about 60 MΩ was then inserted into the ocellar retina through a hole made behind the ocellar lens. A Ag/AgCl wire of 100 µm diameter was inserted into the mesosoma and served as the indifferent electrode. Membrane potentials were recorded through an amplifier (Getting Model 5A, Getting Instruments, San Diego, CA, USA), connected to a computer via a 16-bit data acquisition card (USB-6353, National Instruments, Austin, TX, USA). After penetrating a photoreceptor with the microelectrode, photoreceptor response amplitudes to monochromatic flashes of light were maximized by adjusting the azimuth and elevation of the stimulation fibre. The final position of the optical fibre in visual space was used to define the viewing direction of the stimulated photoreceptor relative to the bee's head, with 0 positioned directly in front of the bee, perpendicular to the dorso-ventral axis of the head. All elevation values for the optical axes of photoreceptors in the median ocellus were corrected to account for the normal head pitch orientation during flight by adding 35 deg (Wehner and Flatt, 1977; see Fig. 4E), so that an optical axis with elevation 0 deg during recording had an elevation of +35 deg relative to the visual horizon after correction for head pitch (see Fig. 4D).

For each photoreceptor, we first determined the spectral sensitivity with a series of 30 ms monochromatic flashes and a temporal spacing of 2 s. Measurements were taken in 20 nm intervals from 340 to 600 nm. The response–stimulus intensity function (V–log I) was recorded over a 4 log unit intensity range at the photoreceptor's peak wavelength sensitivity. The V–log$I$ data were then fitted with the Naka–Rushton equation, $V/V_{max}=I^n/(I^n+K^n)$, where I is the stimulus intensity, V is the response amplitude, V_{max} is the maximum response amplitude, K is the stimulus intensity eliciting 50% of V_{max}, and n is the exponent. Spectral sensitivities were only analysed for recordings where the maximal response amplitude (V_{max}) exceeded 20 mV.

Once the spectral sensitivity of a photoreceptor was established, polarization responses were recorded by placing a UV-transparent linear polarization filter (POL-HNPB-R, Knight Optical, Harrietsham, UK) in front of the optical fibre. Responses to monochromatic flashes at the photoreceptor's peak sensitivity wavelength were recorded at different e-vector orientations. Stimulus intensity was reduced such that the maximum response amplitude did not exceed 50% of V_{max}. e-vector orientation was initially set to 0 (horizontal axis with respect to the dorso-ventral axis of the head) and rotated in 12.5 deg steps to 360 deg. The polarization sensitivity was calculated by relative photon absorption values by applying the V–log$I$ transformation to the recorded data. Relative photon absorption values were then fitted with a sinusoid. PS values were calculated as the ratio of maximum to minimum sensitivity of the fitted sinusoidal curve.

Histology

Histological methods were as described previously (Ribi et al., 2011). Briefly, fully daylight-adapted bees were immobilized by cooling to 4°C. The head capsules were then opened and the tissue was fixed in a mixture of 2% paraformaldehyde and 2.5% glutaraldehyde in phosphate buffer (pH 7.2–7.4) for 2–3 h followed by 2% OsO_4 in distilled water for 1 h. After dehydration and embedding in Araldite (Fluka), semi-thin serial sections of 1 µm thickness were cut with a diamond knife (Diatome). Sections were stained with Toluidine Blue.

The image of a cross-section was imported into Adobe InDesign CS4 (Adobe Systems Incorporated, San Jose, CA, USA) in order to apply lines on straight ocellar rhabdoms. The estimated preferred e-vector orientation of retinular cells is perpendicular to the orientation of these lines, which were exported to a custom-written Matlab program (Mathworks, Natick, MA, USA) for further analysis. In order to map rhabdom density, the cross-section image was imported into ImageJ (Rasband, 1997-2012), rhabdoms were marked and the distribution mapped in a custom-written Matlab program.

A honeybee head was prepared for microCT scan according to Ribi et al. (2008).

Behavioural analysis

Honeybees approaching an indoor feeder were filmed from the side with a high-speed digital camera (MotionPro 10k, Redlake MASD, Inc., San Diego, CA, USA) at 500 frames s^{-1} and dorsal and ventral head coordinates extracted frame-by-frame using a Matlab program (courtesy of Robert Parker and Jan Hemmi, The Australian National University; Mathworks).

Statistical analysis

To test whether the PS values differed according to photoreceptor spectral class, preferred e-vector orientation or ocelli type, a linear mixed model using the maximum likelihood (ML) was implemented in the nlme package of R (https://CRAN.R-project.org/package=nlme). The individual components of variation between bees (bee identity)

Journal of Experimental Biology

Journal of Experimental Biology (2017) 220, 1701-1708 doi:10.1242/jeb.156109

were accounted for by incorporating animal identity as a random effect. Spectral class, preferred e-vector orientation and their interaction were added as fixed effects. A model was constructed by sequentially fitting parameters. Only parameters that were significant at a 5% level when compared with the final model were included in the model. Final residuals were checked graphically for compliance with model assumptions. The linear mixed model using the ML was also used for testing whether the spectral sensitivity peaks differed according to ocelli type.

Statistical significance of differences between preferred e-vector orientation of photoreceptors of different spectral classes or different retinal position were determined by using a permutation approach where the main effect variable was randomly permuted 10,000 times. Permutation was limited to within ocelli to account for the repeated measures structure of the data.

RESULTS

We performed intracellular recordings from 121 photoreceptors of both median and lateral ocelli in 43 honeybee foragers, in order to identify the relationship between the spectral and polarization sensitivity of receptors as well as the direction of their optical axis in the visual field. We confirm that the UV and the green photoreceptors have different polarization sensitivities. Also, the preferred polarization orientations of photoreceptors are significantly different in the dorsal and the ventral retina.

Spectral sensitivity of photoreceptors in the median and the lateral ocelli of honeybees

For each photoreceptor, we firstly determined its spectral sensitivity through a series of equal quanta monochromatic flashes from 340 to 600 nm. Based on these spectral sensitivity profiles, photoreceptors were classified as either UV (N=61) or green receptors (G, N=60), with peak sensitivities at 360 and 500 nm, respectively (Fig. 1A). UV photoreceptors did not show any secondary peak sensitivity at longer wavelengths. There was no difference in spectral sensitivity between the median and the lateral ocelli (P=0.43, linear mixed model).

UV receptors have a higher polarization sensitivity than green receptors

Each spectrally classified photoreceptor was subsequently tested with a series of different e-vector orientations of polarized light by rotating a linear polarizer with flashes at the receptor's peak wavelength sensitivity. The response amplitudes changed depending on the e-vector orientation (0–360 deg, 12.5 deg apart) in a sinusoidal fashion in both UV and green receptors (Fig. 1B). The magnitude of polarization sensitivity of each photoreceptor was calculated as PS values. Most of the green receptors had a PS value of around 2, whereas the UV receptors showed higher PS values and were much more variable (Fig. 2). Average PS values were significantly higher in UV receptors (PS=3.8±1.5) than in green receptors (PS=2.1±0.6) in both median and lateral ocelli (P<0.0001; Table 1). Differences in PS values between median and lateral ocelli just failed to reach significance (P<0.06) with the median ocelli being slightly higher than the lateral ocelli.

Differences in preferred e-vector orientations in the dorsal and the ventral visual field

Fig. 3 shows the distribution of the preferred e-vector orientations of UV and green receptors according to the elevation in the visual field of their optical axes. Overall, the preferred e-vector orientations of receptors did not differ between median and lateral ocelli (P<0.28, permutation test on orientations) or between UV and green

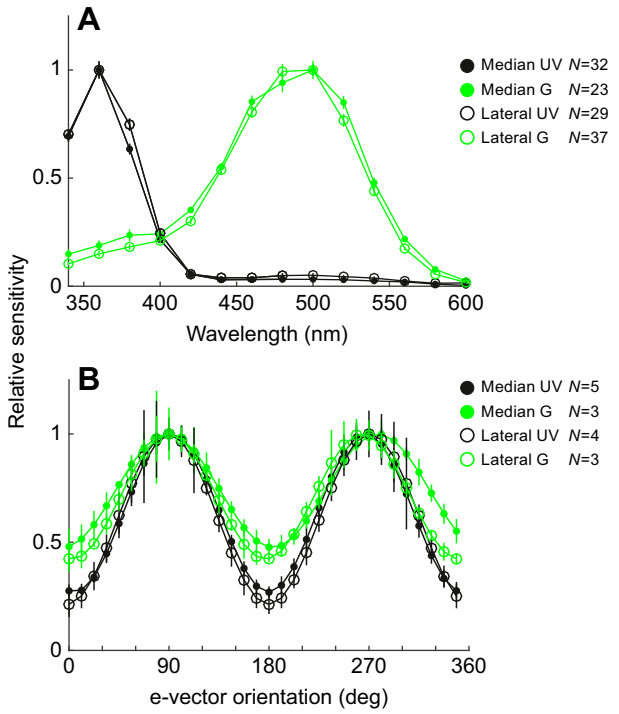

Fig. 1. Spectral and polarization sensitivity of photoreceptors in honeybee ocelli as determined by intracellular recordings. Data are means±s.e.m. (N, sample number). (A) Two types of photoreceptors with peak spectral sensitivity (λ_{max}) at 360 nm (UV, black lines) and at around 500 nm [green (G), green lines] were present in both median and lateral ocelli. (B) Polarization sensitivity of ocellar photoreceptors changes depending on the e-vector orientation of the stimulation light for both UV and green receptors in the median and lateral ocelli.

receptors (P<0.25, permutation test on orientations). However, photoreceptors receiving light from the ventral visual field (<35 deg relative to horizontal) were mostly sensitive to vertically polarized light (e-vector of about 90 deg), while e-vector sensitivities in the dorsal visual field (>35 deg) were much more variable (P<0.0001, permutation test on variability; Fig. 3B,D). The exact elevation threshold did not matter. Statistically significant values between dorsal and ventral visual fields were found for a large range of separation criteria (elevation 10–60 deg). The maximum

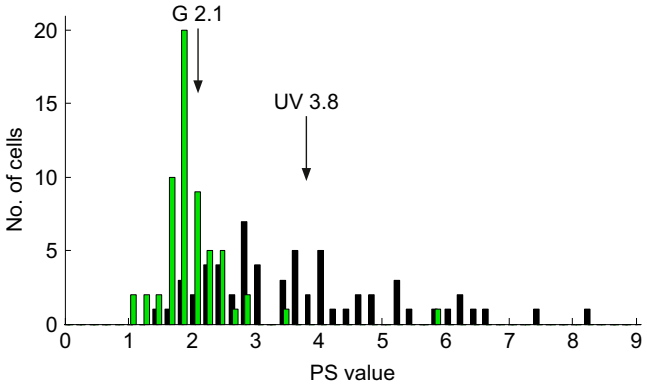

Fig. 2. Polarization sensitivity (PS) values of UV and green photoreceptors in both median and lateral ocelli. The mean PS value was significantly higher in UV (black bars, 3.8±1.5) than in green receptors (green bars, 2.1±0.6; P<0.0001). Differences in PS values between ocelli just failed to reach significance (P<0.06, linear mixed model).

Journal of Experimental Biology (2017) 220, 1701-1708 doi:10.1242/jeb.156109

Table 1. Results of the linear mixed model analysis

Term (added or subtracted from final model)	LLR	*P*-value
Preferred polarization orientation	17.52	0.177
Spectral type	46.19	<0.0001
Median ocelli versus lateral ocelli	3.428	0.064
Region	9.305	0.0023
Region × spectral type interaction	2.297	0.130

Final model in R: Fit=lme (PS value~spectral type+region, random=~1|animal, method='Maximum likelihood'). LLR, log-likelihood ratio. Region, factor indicating dorsal or central visual field. Spectral type, factor indicating UV or green photoreceptor.

significance was found if we used 35 deg as the criterion separating the dorsal and ventral visual fields (Fig. 3A,C). These results indicate clear regional differences in the distribution of preferred e-vector orientations across the ocellar retinae.

Anatomical estimates of rhabdom orientations across the retina

As shown previously for honeybee ocelli (Ribi et al., 2011) and for the blue-banded bees, *Amegilla holmessi* (Zeil et al., 2014), ocellar retinae are divided into a dorsal and a ventral part (Fig. 4A). Here, we are interested in the distribution of the preferred e-vector orientation of rhabdoms in these two retinal compartments. Mapping 183 rhabdoms in a light microscopy cross-section of the retina of the lateral ocellus and measuring the orientation of their elongated cross-sections (Fig. 4B) revealed an area of highest rhabdom density (Fig. 4B, yellow arrow, Fig. 4C) located at a cusp-shaped indentation of the dorsal retina (Fig. 4A, yellow arrow) in which the distal tips of rhabdoms are closest to the focal plane of the lens (Ribi et al., 2011; Hung and Ibbotson, 2014) suggesting that they form an acute zone (Fig. 4C). The rhabdoms in this area of the dorsal retina are particularly long (Fig. 4A), and mainly horizontally elongated in cross-section (Fig. 4B). They are thus likely to be most sensitive to vertically polarized light. Overall, the cross-sections of rhabdoms across the ventral retina form a fan-shaped distribution with a broad range of orientations although the ventral-most rhabdoms appear to be predominantly vertically oriented.

At this stage, unfortunately, we cannot be certain how the visual fields of honeybee ocelli are oriented relative to the visual scene at cruising flight speeds. Head roll orientation, which mainly affects

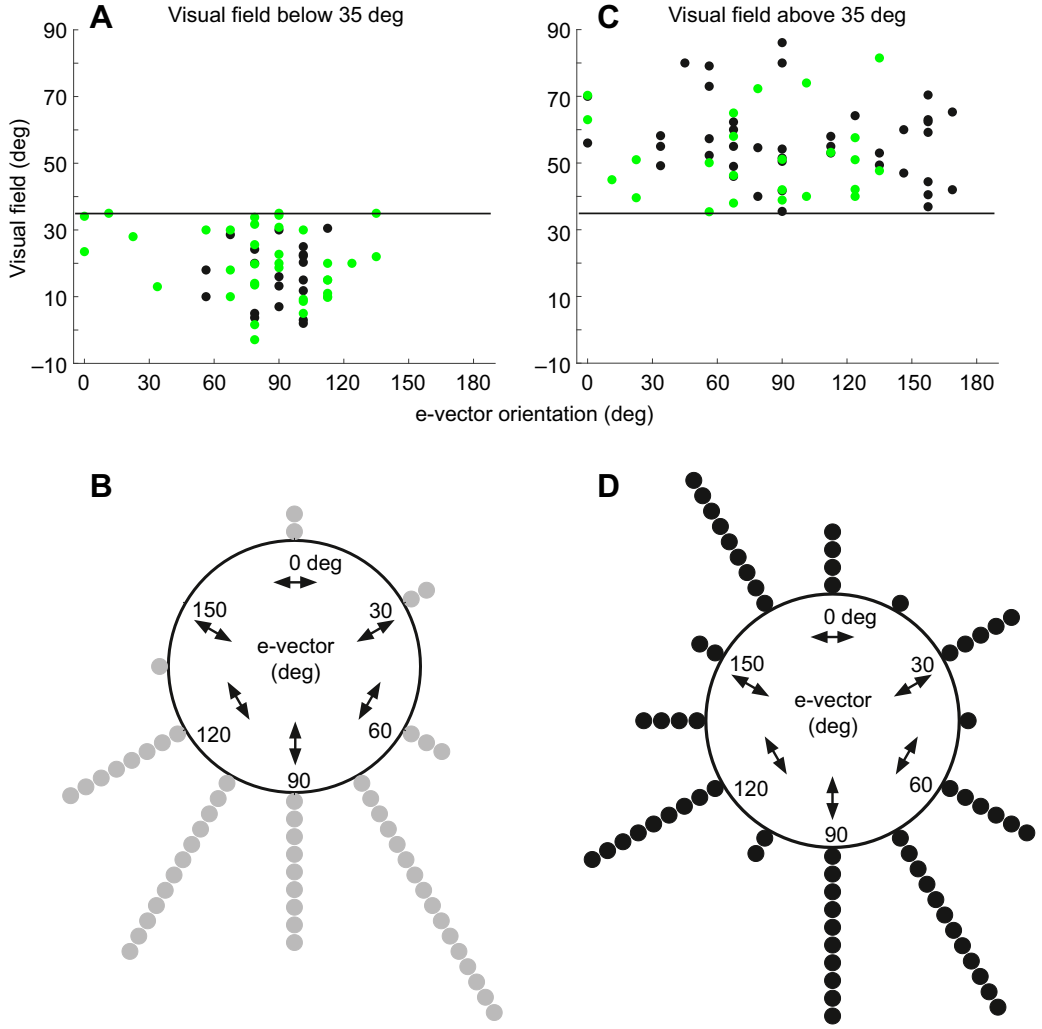

Fig. 3. The preferred e-vector orientation of photoreceptors depends on the direction of their optical axis, as determined by intracellular recordings. (A,B) Photoreceptors receiving light from the ventral visual field below 35 deg. (C,D) Photoreceptors receiving light from the dorsal visual field above 35 deg. In A and C, black dots indicate individual UV cells; green dots are individual green receptors. The circular histograms in B and D show preferred e-vector orientations of ventral visual field receptors (B) and dorsal visual field receptors (D). Significant differences between receptors with dorsal and ventral optical axes were found for a large range of elevation separation criteria (10–60 deg, $P<0.0001$).

Journal of Experimental Biology (2017) 220, 1701-1708 doi:10.1242/jeb.156109

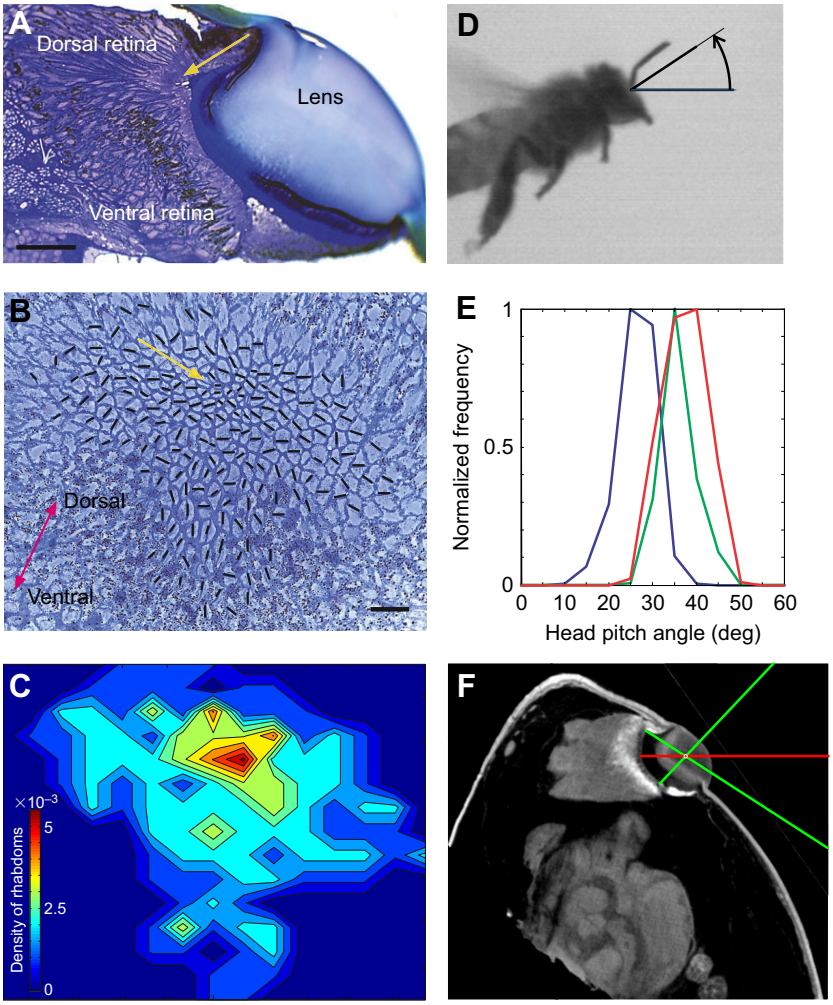

Fig. 4. Orientation of ocelli in the honeybee head and head pitch orientation in flight. (A) Frontal light microscopy section of a lateral ocellus. Scale bar, 50 μm. (B) Light microscopy cross-section of the retina. Black lines indicate the long axis of rhabdom cross-sections in a lateral ocellus. Scale bar, 20 μm. (C) Frequency density plot of rhabdom numbers in the cross-section shown in B. Yellow arrows in A and B indicate the location of the region of the highest photoreceptor density (for further details, see Ribi et al., 2011). (D) Head pitch orientation in free flight (still image from high-speed video footage). (E) Distribution of head-pitch orientation determined every 4 ms for three different bees (marked by different colours) approaching an indoor feeder. (F) Midline sagittal section from a microCT scan of a honeybee worker head, showing the orientation of the median ocellus when the head is tilted backwards by 35 deg. High-speed video footage courtesy of Norbert Boeddeker, University of Bielefeld, Germany.

the orientation of the visual fields of lateral ocelli, is kept perfectly horizontal during flight (Boeddeker and Hemmi, 2010), probably independent of flight speed. This may be different for head pitch orientation, but data are only available for bees approaching a landing site relatively slowly. Wehner and Flatt (1977) found head orientation to be tilted backwards by 20 deg relative to the vertical in this situation. We confirmed this by using high-speed footage of bees approaching an indoor feeder (Fig. 4D), but we also found that head pitch orientation differed widely between bees (Fig. 4E), possibly related to differences in flight speed. In the absence of a systematic analysis of head pitch orientation at different and especially at cruising flight speeds in honeybees, we applied an average value of 35 deg (see Fig. 4E) to correct the viewing angle of photoreceptors in median ocelli (see Materials and methods). A midline sagittal section through a microCT scan of a honeybee median ocellus, tilted backwards by 35 deg (Fig. 4F), suggests that at this head orientation the acute zone of the median ocellar retina views the horizon.

Applying an arbitrary line, we divided rhabdoms into a dorsal and a ventral group to compare the estimated preferred e-vector orientations of their contributing photoreceptors with our electrophysiological results (compare electrophysiology results in Fig. 3B,D with histological results in Fig. 5B,D). By estimating preferred e-vector orientations from the orientation of microvilli (which are aligned perpendicular to the long axis of rhabdom cross-sections emphasized by black lines in Fig. 5A,C), we found a significant difference (P<0.0001, permutation test on variability) between receptors in the dorsal retina (Fig. 5A), which are predicted to be predominantly sensitive to vertically polarized light (compare with Fig. 3B), and receptors in the ventral retina, which are predicted to be sensitive to a wider range of e-vector orientations (compare Figs 5D and 3D). As for the anatomical results, the exact position of the threshold line separating the dorsal and the ventral retinae (Fig. 5A,C) did not matter. Statistically significant values between dorsal and ventral retinae were found for a large range of separation criteria (Fig. S1). The distribution of e-vector orientation sensitivity, as estimated from the anatomy, did not significantly differ from the distribution found in the electrophysiological experiment (see Fig. 3; physiology versus histology in dorsal region, P=0.38; in ventral region P=0.25, permutation test on orientation applied only to the physiological data from lateral ocelli).

DISCUSSION

We have confirmed here that there are two classes of ocellar photoreceptors in honeybee workers with peak wavelength sensitivities at 360 and 500 nm and that the UV receptors have on average higher polarization sensitivities compared with the green receptors. Our work goes beyond earlier studies by demonstrating differences in the distribution of polarization sensitivities in the dorsal and the ventral ocellar retinae and showing that the orientations of elongated rhabdom cross-sections reflect this distribution.

Journal of Experimental Biology (2017) 220, 1701-1708 doi:10.1242/jeb.156109

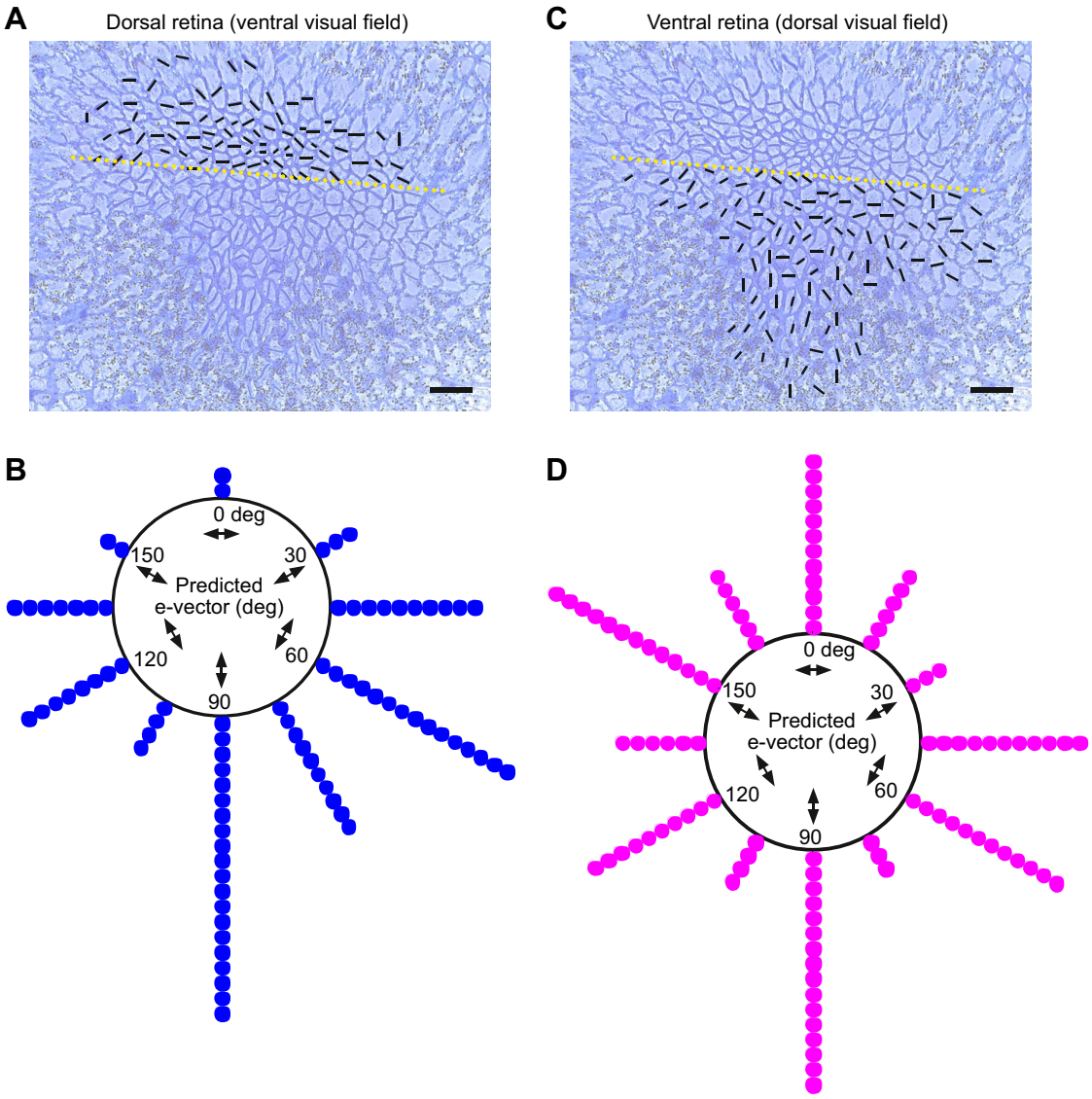

Fig. 5. The orientation of elongated rhabdom cross-sections depends on whether they lie in the dorsal retina and view the ventral visual field (left) or lie in the ventral retina and view the dorsal visual field (right). (A,C) Black lines indicate the long axis of elongated rhabdom cross-sections. Dotted yellow line marks an arbitrary line of separation between a dorsal and a ventral part of the retina, the dorsal part containing the area of highest rhabdom density. Scale bar, 20 μm. (B,D) Circular histograms of rhabdom cross-section orientations. Dots indicate individual rhabdoms. The distribution of rhabdom orientations was significantly different between the dorsal and the ventral part of the retina (P<0.0001).

Two spectrally distinct receptors in ocelli

The results from our intracellular recordings confirm previous electrophysiological studies characterizing spectral sensitivities in honeybee ocelli (Goldsmith and Ruck, 1958; Geiser and Labhart, 1982). However, Geiser and Labhart (1982) identified UV receptors that have a secondary peak at 490 nm, which we did not find. In addition, they described in nine out of 12 UV cells angular sensitivity functions that were bi-modal in elevation with 12.8 ±4.1 deg half-width of the individual peaks, while the other three UV receptors showed a uni-modal angular sensitivity with 10±3 deg half-width (Geiser and Labhart, 1982). Although we did not determine the detailed angular sensitivity characteristics of our cells, we offer the following explanation for Geiser and Labhart's (1982) results: the elongated rectangular profile of rhabdom cross-sections in honeybee ocelli (Ribi et al., 2011) is unlikely to produce bi-modal angular sensitivity functions, but the fact that Geiser and Labhart (1982) also found a secondary peak at around 490 nm in the UV receptor spectral sensitivity indicates that their recordings may have included activity from neighbouring green receptors.

The UV and green receptor sensitivities in honeybee ocelli can be attributed to two opsins, a short-wavelength opsin AmUVop and an ocelli-specific long-wavelength opsin AmLop2, respectively (Velarde et al., 2005). The green receptor in compound eyes, expressing another long-wavelength opsin AmLop1, is maximally sensitive at around 550 nm (Peitsch et al., 1992; Kevan et al., 2001). It has been suggested that UV–green contrast is highly effective for detecting the contrast between the sky and the terrestrial horizon line (Wilson, 1978; Möller, 2002; Kollmeier et al., 2006; Basten and Mallot, 2010; Stone et al., 2014) and the ocellar green receptor with a peak sensitivity shifted toward shorter wavelengths might contribute to sharpen this contrast by increasing its overlap with UV receptors. Some large ocellar interneurons (L-neurons) in honeybees have two spectral sensitivity peaks at 340 and at 500 nm, implying that these cells receive input from both types of

photoreceptor (Milde, 1984). This indicates that this class of neurons cannot provide signals depending on UV–green contrast, while their absolute sensitivity must be improved by the convergence of UV and green receptors. However, Milde (1984) also suggested the possibility of a spectral 'specialist' receiving input from only one photoreceptor type, as has been found in locusts (Wilson, 1978), because his spectral sensitivity investigations did not include all types of L-neuron. It remains to be seen whether such spectral 'specialist' interneurons do exist in honeybees that would be a crucial part of a system providing the UV–green contrast for detecting the terrestrial horizon line.

The polarization sensitivity of UV and green receptors

Our results show that the UV receptors have on average a higher polarization sensitivity (PS=3.8±1.5) compared with green receptors (PS=2.1±0.6). In this context, it is interesting to ask whether the difference in polarization sensitivity between UV and green receptors is due to differences in rhabdom cross-section straightness or to differences in the alignment of photopigment molecules within the microvilli membrane. The magnitude of polarization sensitivity is primarily determined by the rhabdom structure. If a photoreceptor contains microvilli of a constant orientation, the receptor would have a strong e-vector preference, because incident light is absorbed maximally when its e-vector orientation is parallel to the long axis of microvilli (Moody and Parriss, 1961). The cross-sections of ocellar rhabdoms in honeybees are much straighter than those in the nocturnal bee *Megalopta* (Ribi et al., 2011), in which ocellar photoreceptors have been found not to be polarization sensitive (Berry et al., 2011). The maximum predicted PS value that is achievable from perfectly aligned microvilli but with randomly oriented opsin molecules within microvilli falls between 1.6 and 2.0 (Snyder and Laughlin, 1975). We can conclude that visual pigment molecules must be aligned non-randomly with a bias to being parallel to the long axis of the microvilli in UV receptors. In contrast, they are likely to be randomly oriented in green receptors. The enhanced polarization sensitivity of ocellar UV photoreceptors might reflect the fact that scattered skylight is polarized most strongly at short wavelengths (e.g. Snyder, 1973; Lynch and Livingston, 1995). The enhanced polarization sensitivity of ocellar UV photoreceptors thus will increase the UV–green contrast between the terrestrial panorama and the sky even further.

The average PS value of ocellar UV receptors (PS=3.8±1.5) is lower compared with that of UV receptors in the dorsal rim (DRA) of the compound eye, which have an average PS of 6.6 (Labhart, 1980). This is despite the fact that the two receptors express the same short-wavelength opsin AmUVop (Velarde et al., 2005). The difference in PS values of two different UV receptors may be due to differences in rhabdom size, because the smaller the diameter of the rhabdom, the greater the PS as a result of waveguide effects (Snyder, 1973). Ocellar rhabdoms have an average cross-sectional area of 8.7 μm^2 (length 8.7 µm, width 1 µm; Ribi et al., 2011) compared with the cross-sectional areas of rhabdoms in the DRA, which range from 3 to 12 μm^2 (range of diameters: 2–4 µm; Labhart and Meyer, 1999). The long straight cross-sections of ocellar rhabdoms might reflect a need to balance polarization and absolute light sensitivity.

Regional distribution of preferred e-vector orientations

We found that receptors in the dorsal retina receiving light from the ventral visual field (below 35 deg) are mostly sensitive to vertically polarized light, while receptors in the ventral retina viewing the dorsal visual field are sensitive to a wide range of e-vector orientations (Fig. 3) and that this distribution is reflected in the orientations of rhabdom cross-sections.

At this stage, we lack sufficient data on the pitch orientation of the head in honeybees flying at different speeds and so it is difficult to know which part of the ocellar retina is looking at the horizon, although the anatomical division of the retina, with a distinct region of high-density photoreceptors, is very suggestive. However, we found statistically significant differences in rhabdom orientations and polarization sensitivities between dorsal and ventral visual fields applying separation criteria in elevation ranging from 10 to 60 deg. The head pitch orientation in honeybees during cruising flight speeds, when ocellar function is likely to be particularly important, remains to be determined.

Assuming that the region of the highest photoreceptor density in the dorsal ocellus in honeybees (Fig. 4) is aligned with the horizon during flight, it is noteworthy that the photoreceptors in this part of the visual field are predominantly sensitive to vertically polarized light, receive the most focused part of the image (Ribi et al., 2011; Hung and Ibbotson, 2014) and would therefore be able to transmit relatively high spatial frequencies and contrast (Stange et al., 2002; Berry et al., 2007a,b,c; Warrant et al., 2006). In honeybees, four out of five large descending neurons (L-neurons) in the lateral ocelli restrict most of their dendrites to the dorsal retina (Hung and Ibbotson, 2014) and thus include the region of highest photoreceptor density. One out of four L-neurons in the lateral ocelli sends fine dendrites into the border area between the ventral and dorsal retina of the median ocellus (Hung and Ibbotson, 2014) and thus provides a pathway to compare 'equatorial' inputs from the forward-looking median and the two sideways-looking lateral ocelli for the control of roll and pitch orientation of the head. In addition, it is worth noting that because skylight polarization is not uniform along the horizon (except at midday, with the sun close to the zenith), the relative absorption of photons in the polarization-sensitive ocellar photoreceptors will change dramatically as a bee changes her heading direction, i.e. her orientation around the yaw axis (Zeil et al., 2014). Therefore, regardless of where they look, the array of ocellar photoreceptors also provides information about compass direction.

The receptors located in the ventral retina receive light from the sky in both the median and the lateral ocelli. They appear to receive an under-focused image that would be most suited for the detection of small changes of light intensity integrated over a wide visual field (Schuppe and Hengstenberg, 1993; Mizunami, 1995; Berry et al., 2007a,b). The wide range of e-vector sensitivities in the ventral retina if averaged would indeed contribute to boosting photon absorption but averaging would also destroy the polarization information. Among five large descending neuron pairs (L-neurons), only one neuron sends fine branches into the ventral retina of the lateral ocelli (Hung and Ibbotson, 2014). However, the axons of ventral photoreceptors connect to a large number of small interneurons with axon diameters between 2 and 4 µm (Ribi et al., 2011) that may be able to represent, rather than average out, the distribution of preferred e-vector orientations of ventral ocellar photoreceptors.

In conclusion, the distribution of polarization sensitivities across the visual fields of honeybee ocelli suggests that ocelli serve two functions, one is contrast enhancement of the visual horizon for head attitude control and the other is support for the celestial compass system (reviewed in Ribi et al., 2011; Zeil et al., 2014; Taylor et al., 2015). It will thus be interesting in future to study the polarization sensitivities of ocellar interneurons, depending on their dendritic catchment and their size.

Acknowledgements
We thank Dr Yu-Shan Hung for teaching us her technique to handle bees and Dr Norbert Boeddeker for allowing us to use his high-speed footage of honeybees.

Competing interests
The authors declare no competing or financial interests.

Author contributions
Y.O.: Contributed to all stages of the project; W.R.: Performed the anatomical experiments and helped identify and define the problem and revised the manuscript; J.Z.: Performed the behavioural analysis, participated in interpretation of the data and revised the manuscript; J.M.H.: Helped identify and define the problem, participated in data analysis, revised the manuscript and provided funding.

Funding
This study was supported by a Japan Society for the Promotion of Science (JSPS) Postdoctoral Fellowship for Research Abroad to Y.O. and an Australian Research Council grant (FT110100528) to J.M.H.

Supplementary information
Supplementary information available online at
http://jeb.biologists.org/lookup/doi/10.1242/jeb.156109.supplemental

References

Basten, K. and Mallot, H. A. (2010). Simulated visual homing in desert ant natural environments: efficiency of skyline cues. *Biol. Cybern.* **102**, 413-425.
Berry, R. P., Stange, G., Olberg, R. and van Kleef, J. (2006). The mapping of visual space by identified large second-order neurons in the dragonfly median ocellus. *J. Comp. Physiol. A* **192**, 1105-1123.
Berry, R. P., Stange, G. and Warrant, E. J. (2007a). Form vision in the insect dorsal ocelli: an anatomical and optical analysis of the dragonfly median ocellus. *Vision Res.* **47**, 1394-1409.
Berry, R. P., Warrant, E. J. and Stange, G. (2007b). Form vision in the insect dorsal ocelli: an anatomical and optical analysis of the Locust Ocelli. *Vision Res.* **47**, 1382-1393.
Berry, R. P., van Kleef, J. and Stange, G. (2007c). The mapping of visual space by dragonfly lateral ocelli. *J. Comp. Physiol. A* **193**, 495-513.
Berry, R. P., Wcislo, W. T. and Warrant, E. J. (2011). Ocellar adaptations for dim light vision in a nocturnal bee. *J. Exp. Biol.* **214**, 1283-1293.
Boeddeker, N. and Hemmi, J. M. (2010). Visual gaze control during peering flight manoeuvres in honeybees. *Proc. R. Soc. B Biol. Sci.* **277**, 1209-1217.
Fent, K. and Wehner, R. (1985). Oceili: a celestial compass in the desert ant *Cataglyphis*. *Science.* **228**, 192-194.
Geiser, F. X. and Labhart, T. (1982). Electrophysiological investigation on the ocellar retina of the honeybee (*Apis mellifera*). *Verhandlungen der Dtsch. Zool. Gesellschaft* **75**, 307.
Goldsmith, T. H. and Ruck, P. R. (1958). The spectral sensitivities of the dorsal ocelli of cockroaches and honeybees. *J. Gen. Physiol.* **41**, 1171-1185.
Hung, Y.-S. and Ibbotson, M. R. (2014). Ocellar structure and neural innervation in the honeybee. *Front. Neuroanat.* **8**, 1-11.
Kevan, P. G., Chittka, L. and Dyer, A. G. (2001). Limits to the salience of ultraviolet: lessons from colour vision in bees and birds. *J. Exp. Biol.* **204**, 2571-2580.
Kollmeier, T., Röben, F., Schenck, W. and Möller, R. (2006). Spectral contrasts for landmark navigation. *J. Opt. Soc. Am. A* **24**, 1-10.
Kral, K. (1978). The orientation of the rhabdoms in the ocelli of *Apis mellifera carnia* Pollm. and of *Vespa vulgaris* L. *Zoologisches Jahrbuch Physiologie* **82**, 263-271.
Labhart, T. (1980). Specialized photoreceptors at the dorsal rim of the honeybee's compound eye: polarizational and angular sensitivity. *J. Comp. Physiol. A* **141**, 19-30.
Labhart, T. and Meyer, E. P. (1999). Detectors for polarized skylight in insects: a survey of ommatidial specializations in the dorsal rim area of the compound eye. *Microsc. Res. Tech.* **47**, 368-379.
Lynch, D. K. and Livingston, W. (1995). *Color and Light in Nature*. Cambridge: Cambridge University Press.
Milde, J. J. (1984). Ocellar interneurons in the honeybee-structure and signals of L-neurons. *J. Comp. Physiol. A* **154**, 683-693.
Mizunami, M. (1995). Information processing in the insect ocellar system: comparative approaches to the evolution of visual processing and neural circuits. *Adv. Insect Physiol.* **25**, 151-265.
Möller, R. (2002). Insects could exploit UV-green contrast for landmark navigation. *J. Theor. Biol.* **214**, 619-631.
Moody, M. F. and Parriss, J. R. (1961). The discrimination of polarized light by Octopus: a behavioural and morphological study. *Z. Vgl. Physiol.* **44**, 268-291.
Mote, M. I. and Wehner, R. (1980). Functional characteristics of photoreceptors in the compound eye and ocellus of the desert ant, *Cataglyphis bicolor*. *J. Comp. Physiol. A* **137**, 63-71.
Peitsch, D., Fietz, A., Hertel, H., de Souza, J., Ventura, D. F. and Menzel, R. (1992). The spectral input systems of hymenopteran insects and their receptor-based colour vision. *J. Comp. Physiol. A* **170**, 23-40.
Rasband, W. S. (1997-2012). *ImageJ. U. S. National Institutes of Health*. Maryland, USA: Bethesda. http://imagej.nih.gov/ij/.
Ribi, W., Senden, T. J., Sakellariou, A., Limaye, A. and Zhang, S. (2008). Imaging honey bee brain anatomy with micro-X-ray-computed tomography. *J. Neurosci. Methods* **171**, 93-97.
Ribi, W., Warrant, E. and Zeil, J. (2011). The organization of honeybee ocelli: regional specializations and rhabdom arrangements. *Arthropod Struct. Dev.* **40**, 509-520.
Schuppe, H. and Hengstenberg, R. (1993). Optical properties of the ocelli of *Calliphora erythrocephala* and their role in the dorsal light response. *J. Comp. Physiol. A* **173**, 143-149.
Snyder, A. W. (1973). Polarization sensitivity of individual retinula cells. *J. Comp. Physiol.* **83**, 331-360.
Snyder, A. W. and Laughlin, S. B. (1975). Dichroism and absorption by photoreceptors. *J. Comp. Physiol.* **100**, 101-116.
Stange, G. (1981). The ocellar component of flight equilibrium control in dragonflies. *J. Comp. Physiol. A* **141**, 335-347.
Stange, G., Stowe, S., Chahl, J. S. and Massaro, A. (2002). Anisotropic imaging in the dragonfly median ocellus: a matched filter for horizon detection. *J. Comp. Physiol. A* **188**, 455-467.
Stone, T., Mangan, M., Ardin, P. and Webb, B. (2014). Sky segmentation with ultraviolet images can be used for navigation. *Robot. Sci. Syst.* **10**, 47.
Taylor, C. P. (1981). Contribution of compound eyes and ocelli to steering of locusts in flight: I. behavioural analysis. *J. Exp. Biol.* **93**, 1-18.
Taylor, G. J., Ribi, W., Bech, M., Bodey, A. J., Rau, C., Steuwer, A., Warrant, E. J. and Baird, E. (2015). The dual function of orchid bee ocelli as revealed by X-ray microtomography. *Curr. Biol.* **26**, 1-6.
Velarde, R. A., Sauer, C. D., Walden, K. K. O., Fahrbach, S. E. and Robertson, H. M. (2005). Pteropsin: a vertebrate-like non-visual opsin expressed in the honey bee brain. *Insect Biochem. Mol. Biol.* **35**, 1367-1377.
Warrant, E. J., Kelber, A., Wallén, R. and Wcislo, W. T. (2006). Ocellar optics in nocturnal and diurnal bees and wasps. *Arthropod Struct. Dev.* **35**, 293-305.
Wehner, R. and Flatt, I. (1977). Visual fixation in freely flying bees. *Naturwissenschaften* **32c**, 469-471.
Wellington, W. G. (1974). Bumblebee ocelli and navigation at dusk. *Science* **183**, 550-551.
Wilson, M. (1978). The functional organisation of locust ocelli. *J. Comp. Physiol. A* **124**, 297-316.
Zeil, J., Ribi, W. A. and Narendra, A. (2014). Polarisation vision in ants, bees and wasps. In: *Polarized Light and Polarization Vision in Animal Sciences* (ed. G. Horváth), pp. 40-61. Berlin: Springer.

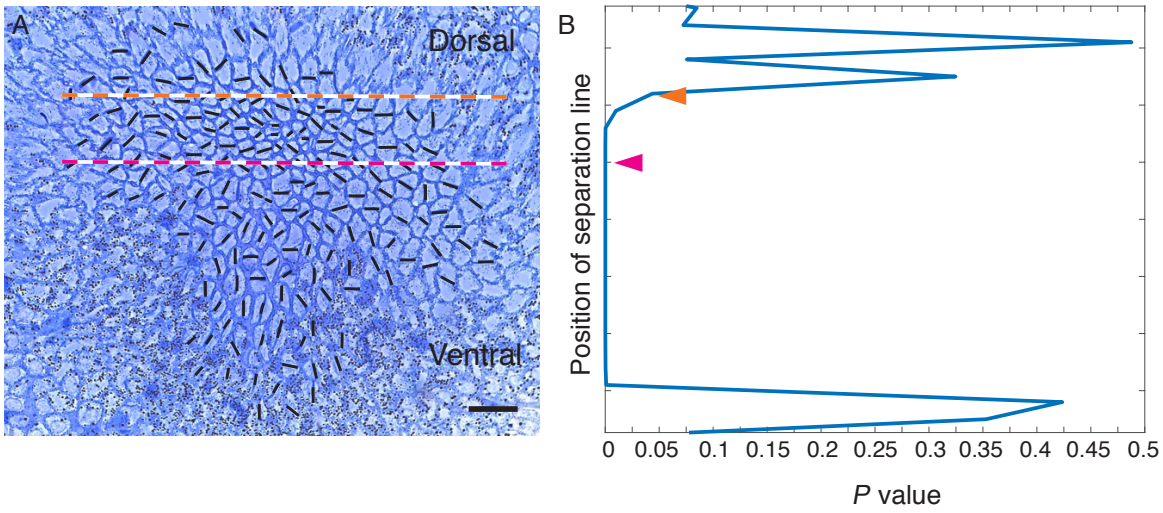

Fig. S1

(A) The orientations of rhabdom cross-section profiles are indicated by black lines in a light microscopy section through the retina of a lateral ocellus. (B) The distribution of rhabdom cross-sections is compared above and below an arbitrary line separating the dorsal and the ventral part of the retina. *P*-values are shown for different positions of this separation line (see arrows in (B) corresponding to lines shown in (A). The orange line in (A) and the orange arrow in (B) indicate the criterion location for which dorsal and ventral distributions are first significant when moving the separation from dorsal to ventral across the retina. The magenta line and arrow show the criterion used in Fig. 5. Dorsal and ventral distributions of rhabdom orientations differ for a large range of positions of the arbitrary separation line.